Equilibrium switching and mathematical properties of nonlinear interaction networks with concurrent antagonism and self-stimulation

Jomar Fajardo Rabajante[a,b,*], Cherryl Ortega Talaue[a]

[a] *Institute of Mathematics, University of the Philippines Diliman, Quezon City, 1101 Philippines*
[b] *Institute of Mathematical Sciences and Physics, University of the Philippines Los Baños, Laguna, 4031 Philippines.*

Abstract

Concurrent decision-making model (CDM) of interaction networks with more than two antagonistic components represents various biological systems, such as gene interaction, species competition and mental cognition. The CDM model assumes sigmoid kinetics where every component stimulates itself but concurrently represses the others. Here we prove generic mathematical properties (e.g., location and stability of steady states) of n-dimensional CDM with either symmetric or asymmetric reciprocal antagonism between components. Significant modifications in parameter values serve as biological regulators for inducing steady state switching by driving a temporal state to escape an undesirable equilibrium. Increasing the maximal growth rate and decreasing the decay rate can expand the basin of attraction of a steady state that contains the desired dominant component. Perpetually adding an external stimulus could shut down multi-stability of the system which increases the robustness of the system against stochastic noise. We further show that asymmetric interaction forming a repressilator-type network generates oscillatory behavior.

Keywords: biological switch, regulatory network, competition, relative dominance regime, multi-stability, oscillations
2000 MSC: 34C60, 92B05
PACS: 87.10.Ed, 87.18.Cf

Highlights

1. Properties of n-dimensional decision model of competitive interaction networks.
2. Graphical technique for component-wise and steady state stability analysis.
3. Search for parameter conditions that control equilibrium switching.
4. Illustrations of multi-stable systems and repressilators.

Graphical Abstract

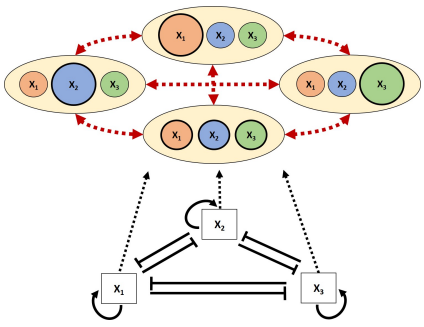

1. Introduction

Mathematical analysis of interaction networks are valuable in understanding the dynamics of complex systems [1, 2, 3, 4, 5]. Concurrent antagonism, where every component of the system simultaneously represses each other, is one of the interaction systems that approximate many natural phenomena. This type of interaction can be observed from gene regulation [6, 7, 8, 9, 10, 11] to mental processes and community structures [12, 13, 14, 15, 16]. The concurrent decision-making model (CDM), which was originally proposed by Cinquin and Demongeot [17], represents the mutual antagonistic interaction among components. The characteristics (e.g., initial condition, growth and decay) of each component and the strength of inter-component repression decide what component eventually dominates the system [18, 19, 20].

We study the mathematical properties of the CDM where a component of the system can denote any inhibiting factor (e.g., protein, species, mental choice) as long as the interaction among the components follows the network shown in Figure (1). Molecular, ecological and cognitive interaction networks in the same layout as Figure (1) can be abstractly described by the CDM, similar to the classical competitive models (e.g., Lotka-Volterra) that have been used to represent various chemical reactions and population dynamics [21]. Furthermore, it is assumed that each component stimulates itself and the kinetics describing the gross growth rate of each component follows a non-polynomial sigmoid curve. The self-stimulation rate in the CDM model serves as a positive-feedback memory.

*Corresponding author. Phone number: +63 49 536-6610. Present address: Graduate School of Science and Technology, Shizuoka University, 3-5-1 Johoku, Naka-ku, Hamamatsu City, 432-8561 Japan.
Email addresses: jfrabajante@up.edu.ph (Jomar Fajardo Rabajante), cherryl@math.upd.edu.ph (Cherryl Ortega Talaue)

Self-stimulation is a common property of master switches in gene regulation and other biological signaling systems [22, 17, 23, 24]. In fact, the CDM is a candidate model of biological switches that exhibit multi-stability (co-existence of multiple stable equilibria) [25, 26, 27, 28, 29]. At the ecological level, self-stimulation can be regarded as a characteristic of individuals or populations for increasing fitness and avoiding extinction. The non-polynomial CDM is an alternative to the classical polynomial models, especially when such polynomial models do not replicate the nonlinear effect of antagonistic interaction and sigmoidal growth [30, 14, 31, 32, 33, 34].

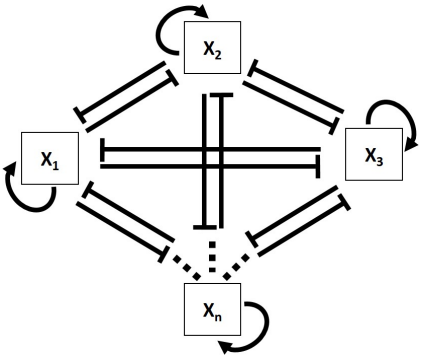

Figure 1: CDM interaction network (adopted from [35, 17]). Bars represent inhibition, while arrows represent stimulation. The nodes represent interacting components of a system.

The CDM network (Fig. (1)) can be a motif that is part of a much larger network [36, 37, 38, 39, 40, 41]. Conversely, the CDM can be used to study various large networks by converting them to coarse-grained networks with self-stimulation loops and concurrent antagonism among modules of sub-networks (see [42] for an example). The qualitative behavior of the dynamics of the CDM can be analyzed by translating the interaction network into a system of ordinary differential equations (ODE). Existing ODE models of CDM have been employed, such as to study cell-fate determination, but only for symmetric interactions [43, 42, 17]. Here, our mathematical results are generalizable for high-dimensional systems (number of components is more than two) and for asymmetric reciprocal antagonism. The model that we analyze has more adjustable parameters to represent a wider range of situations and to predict more types of outcomes (e.g., multi-stable states and oscillation). However, note that the CDM model is not intended to model an exact physical representation of a system, such as the binding of repressors and activators to the DNA, but rather to describe the abstract dynamics of the system (e.g., theoretical characterization of the qualitative behavior of multi-stable decision switches in cell-fate determination).

In this paper, stability and bifurcation analyses of the ODE model are performed by utilizing the geometric properties of the sigmoid kinetics. The analysis focuses on the non-negative real-valued states of the ODE model, and the steady states (equilibrium points) are classified based on the dominance level of its components. A 'desired steady state' refers to the equilibrium point such that the preferred component has the dominant value. We identify how varying the values of some parameters, such as maximal growth rate, effect of external stimuli, decay rate and interaction strength, steer the system toward a desired equilibrium. We search for parameter conditions that control equilibrium switching, which means driving a solution to the ODE model to converge from an undesirable steady state to the desired steady state. Moreover, illustrative examples of several cases (e.g., finite and infinite number of steady states, and oscillations) are presented. This paper is a comprehensive mathematical reference highlighting the general characteristics of the CDM.

2. Model and Methods

A state $X = (X_1, X_2, ..., X_n)$ represents a temporal stage in the CDM. The component (coordinate) X_i of a state represents the value (concentration, population, worth) of the i-th node in the CDM interaction network. A stable steady state $X^* = (X_1{}^*, X_2{}^*, ..., X_n{}^*)$ represents the long-term fate of the system for a certain set of parameter values and initial condition. For example, a steady state may represent a certain cell phenotype in the cell differentiation process, an outcome of competition among species, or a preference from a set of mental choices. The dominant component dictates the expressed gene, the victorious species, or the prevailing choice among conflicting alternatives.

The CDM interaction network with self-stimulation (auto-activation) can be translated to an ODE model as follows:

$$\frac{dX_i}{dt} = F_i(X) = \frac{\beta_i X_i^{c_i}}{K_i + X_i^{c_i} + \sum_{j \neq i} \gamma_{i,j} X_j^{c_{i,j}}} + g_i - \rho_i X_i, \quad (1)$$

$$\text{for } i = 1, 2, ..., n$$

where n is the number of nodes in the network. This ODE model is a generalization of the symmetric ODE model in [17]. We restrict the parameters to be non-negative real numbers. The parameter β_i is the growth constant of the unrepressed X_i relative to the first-order degradation; ρ_i is the assumed first-order degradation or death rate (exponential decay) of X_i; and $\gamma_{i,j}$ is the interaction coefficient associated with the inhibition of X_i by X_j. If $\gamma_{i,j} = 0$ then X_j does not inhibit the growth of X_i. The matrix of interaction coefficients $\left[\gamma_{i,j}\right]$ can be symmetric or asymmetric. Moreover, we consider

$$g_i = e_i + \alpha_i s_i \quad (2)$$

to represent constant basal or constitutive growth (e_i) of X_i [44, 45] plus the effect of the external stimulus with value s_i and rate α_i. In this paper, we assume that g_i is constant.

We define the multivariate sigmoid function H_i by

$$H_i(X_1, X_2, ..., X_n) = \frac{\beta_i X_i^{c_i}}{K_i + X_i^{c_i} + \sum_{j \neq i} \gamma_{i,j} X_j^{c_{i,j}}} \quad (3)$$

PeerJ PrePrints | http://dx.doi.org/10.7287/peerj.preprints.382v3 | CC-BY 4.0 Open Access | rec: 31 Jan 2015, publ: 31 Jan 2015

which is similar to the classical Hill equation [46, 47]. The terms $\sum_{j\neq i}\gamma_{i,j}X_j^{c_{i,j}}$ in the denominator reflect the nonlinear inhibitory influence of other components on the growth of X_i. The parameter $K_i > 0$ is the threshold constant. If all $X_j = 0$ for all $j \neq i$ then the function value of H_i is equal to $\beta_i/2$ when $X_i = K_i^{1/c_i}$. The parameter $c_i \geq 1$ defines the shape and the steepness of the sigmoid curve associated with X_i, and denotes self-stimulation. The parameter $c_{i,j}$, $j \neq i$ affects the strength of inhibition of X_i by X_j. These exponents represent the sigmoid kinetics possibly formed by multiple intrinsic and extrinsic processes affecting the growth of X_i [48]. To clarify some terminologies used in this paper, dX_i/dt is the net growth rate of X_i and we define H_i as the gross growth rate without taking into account the decay of X_i. Throughout this paper, we simply call H_i as growth rate. In addition, the lower bound of H_i (3) is zero and its upper bound is β_i (refer to Remark (1) in the succeeding subsection). Thus, the value $\beta_i + g_i$ can also be interpreted as the maximal growth rate of X_i.

2.1. *Graphical technique for stability analysis*

We can investigate the multivariate sigmoid function (3) by looking at the univariate function defined by

$$H_i^1(X_i) = \frac{\beta_i X_i^{c_i}}{K_i + X_i^{c_i} + \sum_{j\neq i}\gamma_{i,j}X_j^{c_{i,j}}} \tag{4}$$

where each X_j, $j \neq i$ is taken as a dynamic parameter. This means that we project the high-dimensional space onto a two-dimensional plane. If $c_i > 1$, the graph of the univariate function H_i^1 in the first quadrant of the Cartesian plane is sigmoidal for any value of X_j, $j \neq i$. If $c_i = 1$, the graph of the function H_i^1 in the first quadrant is hyperbolic for any value of X_j, $j \neq i$ (although, in this paper, we generally call H_i^1 with $c_i \geq 1$ as sigmoid function). Moreover, when the value of c_i increases, the graph of $Y = H_i^1(X_i)$ gets steeper. If we add a term g_i to $H_i^1(X_i)$ then the graph of $Y = H_i^1(X_i)$ in the Cartesian plane is translated upwards by g_i units.

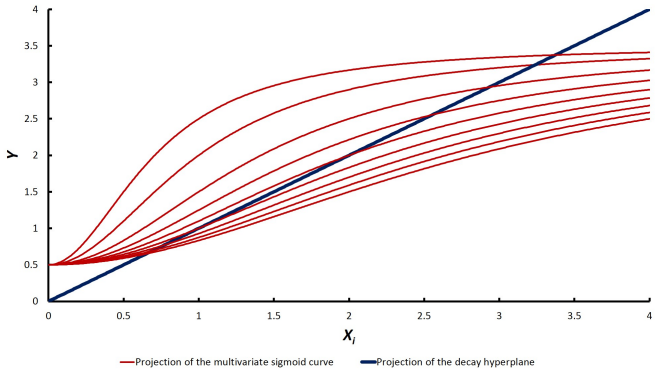

Figure 2: Projection of multivariate sigmoid function and decay hyperplane onto a Cartesian plane. We investigate the intersections of planar $Y = \rho_i X_i$ (line) and $Y = H_i^1(X_i) + g_i$ (sigmoid) with varying values of $\sum_{j\neq i}\gamma_{i,j}X_j^{c_{i,j}}$. Note that an intersection of the line and the sigmoid curve is not necessarily a component of a steady state.

The geometric properties of the sigmoid function is essential in understanding the nature of the steady states. To find the steady states, we need to solve the multivariate equation $F_i(X) = 0$ for all i (where F_i is given in the ODE system (1)). This implies that we need to determine the real solutions to

$$\frac{\beta_i X_i^{c_i}}{K_i + X_i^{c_i} + \sum_{j\neq i}\gamma_{i,j}X_j^{c_{i,j}}} + g_i = \rho_i X_i \text{ for all } i. \tag{5}$$

That is, we identify the intersections of the $n+1$-dimensional curves generated by the multivariate sigmoid function $H_i + g_i$ (left hand side of Equation (5)) and the $n+1$-dimensional decay hyperplane generated by $\rho_i X_i$ (right hand side of Equation (5)). For easier analysis, we rather examine the intersections of the univariate functions defined by $Y = H_i^1(X_i) + g_i$ and $Y = \rho_i X_i$ while varying the value of $\sum_{j\neq i}\gamma_{i,j}X_j^{c_{i,j}}$ in the denominator of the univariate sigmoid function H_i^1 (4) (see Figure (2) for illustration). In the univariate case, we can look at $Y = \rho_i X_i$ as a line in the Cartesian plane passing through the origin with slope equal to ρ_i.

Remark 1. It is always true that

$$\beta_i \geq \frac{\beta_i X_i^{c_i}}{K_i + X_i^{c_i}} \geq \frac{\beta_i X_i^{c_i}}{K_i + X_i^{c_i} + \sum_{j\neq i}\gamma_{i,j}X_j^{c_{i,j}}} \geq 0 \tag{6}$$

for any value of X_j for all j. In fact, if the value of $\sum_{j\neq i}\gamma_{i,j}X_j^{c_{i,j}}$ in the denominator of $H_i^1(X_i)$ increases, then the graph of the sigmoid curve $Y = H_i^1(X_i)$ shrinks (see Figure (2)). Note that each X_j, $j \neq i$ is taken as a dynamic parameter but varying these parameters does not change the sigmoid shape of $Y = H_i^1(X_i)$.

Consequently, one strategy for determining the stability of a steady state for a given set of parameter values is by doing component-wise stability analysis.

Definition 1. *Attracting component.* Suppose X_i^* is the i-th component of X (i.e., $X = (X_1, X_2, ..., X_i^*, ..., X_n)$), where X is not necessarily a steady state. Under the assumption that the value of $\sum_{j\neq i}\gamma_{i,j}X_j^{c_{i,j}}$ in the denominator of the univariate sigmoid function (4) is fixed, if X_i converges to X_i^* for all initial conditions near X_i^*, then we say that the i-th component X_i^* of X is attracting.

Property 1. *The steady state $X^* = (X_1^*, X_2^*, ..., X_n^*)$ of the CDM ODE system (1) is stable only if all its components are attracting. In other words, if at least one of the components of X^* is non-attracting, then X^* is unstable.*

Note that the converse of this statement is not always true (refer to Example (2) in the next section and to Appendix A).

Here is an example to illustrate Property (1):

Example 1. Consider the CDM ODE system (1) with $n = 3$, $\beta_i = 2$, $c_i = c_{i,j} = 3$, $K_i = 1$, $\gamma_{i,j} = 1$ and $\rho_i = 1$, for all $i, j = 1, 2, 3$. Let $g_1 = 0.1$, $g_2 = 0$ and $g_3 = 0$. We want to determine the stability of one of the steady states, $(X_1^* = 0.10103, X_2^* = 1.001, X_3^* = 0)$, by employing Property (1). We

PeerJ PrePrints | http://dx.doi.org/10.7287/peerj.preprints.382v3 | CC-BY 4.0 Open Access | rec: 31 Jan 2015, publ: 31 Jan 2015

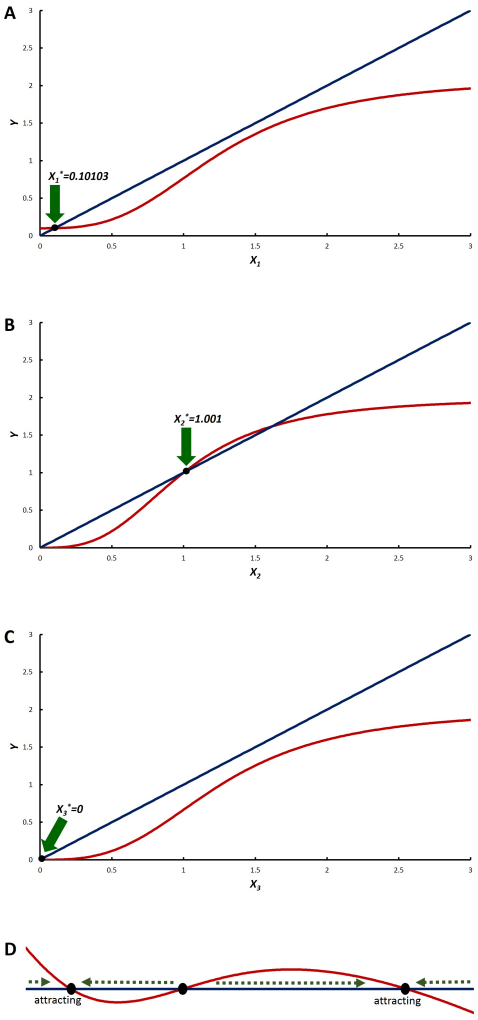

Figure 3: (**A**) Graphs of $Y = H_1^1(X_1) + 1$ and $Y = X_1$ with fixed $X_2 = 1.001$ and $X_3 = 0$ (refer to Example (1)). (**B**) Graphs of $Y = H_2^1(X_2)$ and $Y = X_2$ with fixed $X_1 = 0.10103$ and $X_3 = 0$. (**C**) Graphs of $Y = H_3^1(X_3)$ and $Y = X_3$ with fixed $X_1 = 0.10103$ and $X_2 = 1.001$. (**D**) The curves are rotated making the line $Y = \rho_i X_i$ as the horizontal axis. Positive slope means non-attracting, negative slope means attracting. If the slope is zero, we look at the left and right neighboring slopes.

test if a component is attracting or not by utilizing the geometric properties of the planar curves $Y = H_i^1(X_i) + g_i$ and $Y = \rho_i X_i$, $i = 1, 2, 3$.

The test is done by investigating the components one by one. Examine the intersection of $Y = H_1^1(X_1) + 1$ and $Y = X_1$ with $X_2 = 1.001$ and $X_3 = 0$ (Figure (3A)), then determine if $X_1{}^* = 0.10103$ is attracting using Figure (3D) (see SM5 in the Supplementary Material for the discussion about this criterion). We conclude that $X_1{}^* = 0.10103$ is an attracting component.

Now, test the attraction of $X_2{}^* = 1.001$ by looking at the intersection of $Y = H_2^1(X_2)$ and $Y = X_2$ with $X_1 = 0.10103$ and $X_3 = 0$ (Figure (3B)). Furthermore, test $X_3{}^* = 0$ by looking at the intersection of $Y = H_3^1(X_3)$ and $Y = X_3$ with $X_1 = 0.10103$ and $X_2 = 1.001$ (Figure (3C)). The tests reveal that $X_2{}^* = 1.001$ is non-attracting and $X_3 = 0$ is attracting.

Therefore, the equilibrium point $(X_1{}^* = 0.10103, X_2{}^* = 1.001, X_3{}^* = 0)$ is unstable because of the presence of a non-attracting component $X_2{}^* = 1.001$.

Note that we can conclude that a steady state is unstable by using Property (1). However, we cannot immediately conclude if a steady state is stable by using component-wise stability analysis. There are exceptions where some unstable steady states have components that are all attracting (see Appendix A.1 for illustration). If the tests are inconclusive, we employ other techniques, such as linearization using Jacobian matrix. The exceptions usually arise when there are oscillating solutions to the CDM ODE model (1).

3. Results and Discussion

In this section, we present several mathematical properties of the CDM ODE model (1). We assume that the initial value, denoted by $X_0 = (X_{1,0}, X_{2,0}, ..., X_{n,0})$, is non-negative real-valued. It follows that the solution to the ODE model (1) is always non-negative. Note that given non-negative state variables and parameters in the ODE system (1), if $g_i > 0$ then $\rho_i > 0$ for every i is a necessary and sufficient condition for the existence of a steady state. For the proofs of the mathematical properties and additional illustrations, see the supporting text in the Supplementary Material.

Property 2. *Suppose $\rho_i > 0$. The value $\frac{g_i+\beta_i}{\rho_i}$ is an upper bound of, but will never be equal to, the attracting component $X_i{}^*$. The steady states of the CDM ODE system (1) lie on the hyperspace*

$$\left[\frac{g_1}{\rho_1}, \frac{g_1+\beta_1}{\rho_1}\right) \times \left[\frac{g_2}{\rho_2}, \frac{g_2+\beta_2}{\rho_2}\right) \times ... \times \left[\frac{g_n}{\rho_n}, \frac{g_n+\beta_n}{\rho_n}\right). \qquad (7)$$

Note that if both $g_i > 0$ and $\rho_i > 0$ then $X_i = g_i/\rho_i$ can only be an i-th component of a steady state of the ODE system (1) if $\beta_i = 0$. We can expand the size of the hyperspace (7) by increasing the value of g_i and β_i (maximal growth rate), and by decreasing the value of ρ_i (decay rate). In species competition, this hyperspace limits the carrying capacity of the population.

Property 3. *Suppose $\rho_i > 0$ for all i. Then each component of any state of the CDM ODE model (1) is always attracted by an attracting component. Note that this attraction does not necessarily mean convergence to equilibrium because the value of $\sum_{j\neq i} \gamma_{i,j} X_j^{c_{i,j}}$ in the denominator of the sigmoid function (4) can vary.*

The convergence to a steady state is common to CDM ODE models, especially in systems with symmetric interaction matrix (e.g., $\gamma_{i,j} = \gamma$ for all i, j, γ is a constant). However, note that an attracting component can either be a coordinate of a steady state or an attractor that induces sustained oscillations. The sustained oscillations are due to the varying value of $\sum_{j\neq i} \gamma_{i,j} X_j^{c_{i,j}}$ in the denominator of the sigmoid function that causes continuous change in the intersections of $Y = H_i^1(X_i) + g_i$ and $Y = \rho_i X_i$.

PeerJ PrePrints | http://dx.doi.org/10.7287/peerj.preprints.382v3 | CC-BY 4.0 Open Access | rec: 31 Jan 2015, publ: 31 Jan 2015

Property 4. *Suppose sustained oscillations exist. The value of* $\frac{g_i+\beta_i}{\rho_i}$ *is an upper bound of the sustained oscillating solution to* X_i*. The sustained oscillations of the CDM ODE system (1) are contained in the hyperspace (7).*

Here is an example of a model with oscillating solution:

Example 2. One example of such oscillating system is a repressilator (a type of synthetic biological oscillator [49, 50, 51, 52, 53, 54]) of the form

$$\begin{aligned}\frac{dX_1}{dt} &= \frac{X_1^2}{1+X_1^2+X_2^2+0.1X_3^2} - 0.1X_1 + 0.1 \\ \frac{dX_2}{dt} &= \frac{X_2^2}{1+0.1X_1^2+X_2^2+X_3^2} - 0.1X_2 + 0.1 \\ \frac{dX_3}{dt} &= \frac{X_3^2}{1+X_1^2+0.1X_2^2+X_3^2} - 0.1X_3 + 0.1.\end{aligned} \tag{8}$$

Notice that the reciprocal interaction among components in this example is asymmetric where one direction of inhibition is stronger than the reverse direction (Appendix A.1). According to various mathematical propositions from previous studies, such as the Thomas' rules, positive circuits (e.g., two mutually inhibiting components with symmetric reciprocal repression) induce multi-stability, and negative circuits (e.g., asymmetric inhibition among three components that form a repressilator) induce oscillations [55, 56, 57, 58].

Now, suppose c_i and $c_{i,j}$ are integers for all i and j. The corresponding polynomial equation to

$$F_i(X) = \frac{\beta_i X_i^{c_i}}{K_i + X_i^{c_i} + \sum_{j\neq i} \gamma_{i,j} X_j^{c_{i,j}}} - \rho_i X_i + g_i = 0 \tag{9}$$

is

$$P_i(X) = \beta_i X_i^{c_i} + (g_i - \rho_i X_i)\left(K_i + X_i^{c_i} + \sum_{j\neq i} \gamma_{i,j} X_j^{c_{i,j}}\right) = 0 \tag{10}$$

for all i.

Property 5. *Under the assumption that that there is only a finite number of steady states, the number of steady states of the CDM ODE model (1) (where* c_i *and* $c_{i,j}$ *are integers) is at most*

$$\prod_{i=1}^{n} max\{c_i + 1, c_{i,j} + 1 \text{ for all } j \neq i\}. \tag{11}$$

The proof of Property (5) is by Bézout Theorem [59] applied to the system of polynomial equations (10). Bézout Theorem does not give the exact number of steady states but only the upper bound. From Property (5), the maximum number of steady states is dependent on the value of c_i and $c_{i,j}$ as well as on n (dimension of our state space). Note that the size of the basin of attraction of a steady state depends on the number of existing steady states and on the size of the hyperspace (7). The hyperspace (7) is fixed for a given set of parameter values, and the basin of attraction of each existing steady state is distributed in this hyperspace. If there are multiple stable steady states then there are multiple basins of attraction that share the region of the hyperspace.

3.1. *Classification of stable steady states according to relative dominance*

The following definition of terms are used to classify the steady states based on the dominant component.

Definition 2. *Classification of steady states.* A component is switched-off (inactive or extinct) if its value is zero, and switched-on otherwise. A switched-on X_i dominates X_j if $X_j/X_i < \epsilon \leq 1$, where $\epsilon > 0$ is an acceptable tolerance constant.

- 1-node dominance or premier state refers to the case where a stable steady state has only one dominant component;
- p-node co-dominance or intermediate state refers to the case where a stable steady state has $1 < p < n$ dominant components such that the dominant components have equal positive values; and
- n-node co-dominance or priming state refers to the case where all components of a stable steady state have equal positive values.

Suppose we want the i-th component of a state to be dominant, then we say that X is a *desired steady state* if the component X_i^* of X is dominant.

Here is an example showing the possible types of steady states in a 2-dimensional CDM:

Example 3. Consider the CDM ODE model (1) with $n = 2$, $c_i = c_{i,j} = 1$ and $g_i = 0$, $i, j = 1, 2$. If the number of steady states is finite, then we expect that the maximum number of possible steady states is 4. The possible steady states are

- Zero state (all components are switched-off): $(0, 0)$. This is stable when $\beta_i < \rho_i K_i$, for all $i = 1, 2$.
- One component is switched-on: $\left(0, \frac{\beta_2 - \rho_2 K_2}{\rho_2}\right)$. This is a steady state if $\beta_2 > \rho_2 K_2$, and stable (premier state) if $\beta_1 < \rho_1\left(K_1 + \gamma_{1,2}\frac{\beta_2 - \rho_2 K_2}{\rho_2}\right)$.
- One component is switched-on: $\left(\frac{\beta_1 - \rho_1 K_1}{\rho_1}, 0\right)$. This is a steady state if $\beta_1 > \rho_1 K_1$, and stable (premier state) if $\beta_2 < \rho_2\left(K_2 + \gamma_{2,1}\frac{\beta_1 - \rho_1 K_1}{\rho_1}\right)$.
- All components are switched-on: $\left(\frac{\beta_1 - \rho_1\left(K_1 + \gamma_{1,2}\left(\frac{\beta_2}{\rho_2} - K_2\right)\right)}{\rho_1(1-\gamma_{1,2}\gamma_{2,1})}, \frac{\beta_2 - \rho_2\left(K_2 + \gamma_{2,1}\left(\frac{\beta_1}{\rho_1} - K_1\right)\right)}{\rho_2(1-\gamma_{2,1}\gamma_{1,2})}\right)$.
  This state is stable for a range of parameter values, if it exists. This state satisfies the system of equations generated by
  $\left(\frac{\beta_1 - \rho_1(K_1 + \gamma_{1,2}X_2^*)}{\rho_1}, \frac{\beta_2 - \rho_2(K_2 + \gamma_{2,1}X_1^*)}{\rho_2}\right) = (X_1{}^*, X_2{}^*)$.
  If $X_1{}^* = X_2{}^*$ and $(X_1{}^*, X_2{}^*)$ is stable, then we have a priming state.

PeerJ PrePrints | http://dx.doi.org/10.7287/peerj.preprints.382v3 | CC-BY 4.0 Open Access | rec: 31 Jan 2015, publ: 31 Jan 2015

3.2. Infinitely many steady states and the zero state

There are cases where the polynomial system (10) has infinitely many complex-valued solutions, hence, Property (5) does not apply. Infinitely many steady states (degenerate case) could arise if all equations in the polynomial system (10) have a common factor of degree greater than zero.

Property 6. *Suppose* $c_i = c_{i,j} = 1$, $K_i = K > 0$, $\gamma_{i,j} = 1$, $g_i = 0$, $\beta_i = \beta > 0$ *and* $\rho_i = \rho > 0$ *where* $\beta > \rho K$ *for all* i *and* j (K, β *and* ρ *are constants). Then the polynomial system associated with the CDM ODE model (1) has a non-constant common factor. Any CDM ODE model that can be converted to this type of polynomial system has infinitely many steady states.*

To illustrate Property (6), here is an example:

Example 4. An example of a CDM ODE model having infinitely many equilibrium points is of the form

$$\frac{dX_i}{dt} = \frac{AX_i}{K + X_i + \sum_{j\neq i} X_j} - X_i,\ i = 1, 2, ..., m \tag{12}$$

$$\frac{dX_k}{dt} = \frac{X_k}{K + X_k + \sum_{j\neq k} X_j} - \frac{X_k}{A},\ k = m+1, m+2, ..., n$$

where $A > K$ is a constant (see Figure (4) for illustration). The polynomial system (10) of this CDM ODE model is similar to the polynomial system of the CDM ODE model described in Property (6) with $\beta = A$ and $\rho = 1$.

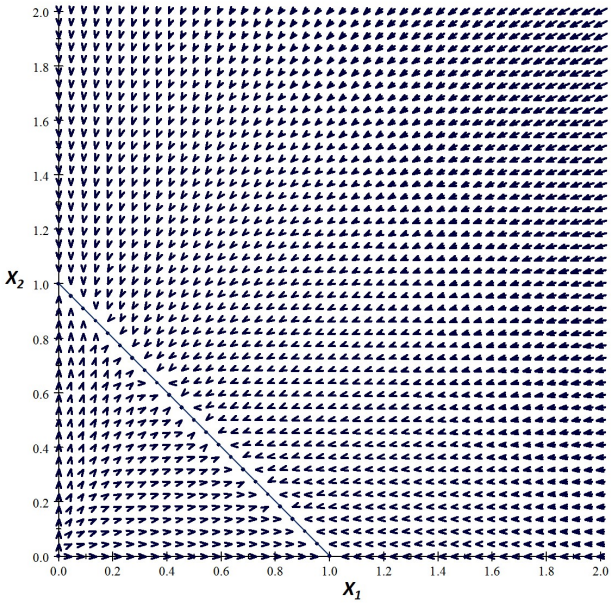

Figure 4: A phase plane showing an attracting line. Parameter values are $n = 2$, $c_1 = c_2 = c_{1,2} = c_{2,1} = 1$, $K_1 = K_2 = 1$, $\gamma_{1,2} = \gamma_{2,1} = 1$, $g_1 = g_2 = 0$, $\beta_1 = 2$, $\beta_2 = 1$, $\rho_1 = 1$ and $\rho_2 = 1/2$.

Property 7. *Suppose* $c_i = c_{i,j} = 1$, $K_i = K > 0$, $\gamma_{i,j} = 1$, $g_i = 0$, $\beta_i = \beta > 0$ *and* $\rho_i = \rho > 0$ *for all* i *and* j (K, β *and* ρ *are constants). If* $\beta > \rho K$ *then the steady states of the ODE system (1) are the zero state and the non-isolated points lying on the hyperplane with equation*

$$\sum_{j=1}^{n} X_j = \frac{\beta}{\rho} - K,\ X_j \geq 0 \text{ for all } j. \tag{13}$$

The zero state is an unstable equilibrium point while the hyperplane (13) is an attractor.

Furthermore, the convergence to the zero state $(0, 0, ..., 0)$ implies that all components eventually switch-off. Note that the CDM ODE model (1) has a steady state with i-th component $X_i^* = 0$ if and only if $g_i = 0$. The zero state of the ODE system (1) can only be a steady state if and only if $g_i = 0$ for all i.

In general, suppose $g_i = 0$ for all i, then we are sure that the zero state is the only equilibrium point of the ODE model (1) if the univariate curve $Y = H_i^1(X_i)$ lies below the decay line $Y = \rho_i X_i$ (i.e., $H_i^1(X_i) < \rho_i X_i$, for all $X_i > 0$) for every $i = 1, 2, ..., n$. This phenomenon indicates that the exponential decay of each component is faster than stimulation, thus, we expect that all components will eventually be switched-off given any initial condition.

Property 8. *If* $c_i > 1$, $g_i = 0$ *and*

$$\rho_i (K_i^{1/c_i}) \geq \beta_i \tag{14}$$

for all i, *then the CDM ODE system (1) has only one equilibrium point which is the zero state because the univariate curve* $Y = H_i^1(X_i)$ *lies below the decay line* $Y = \rho_i X_i$.

In addition, if $c_i = 1$, $g_i = 0$ *and* $\beta_i / K_i \leq \rho_i$ *for all* i, *then the ODE system (1) has the zero state as the sole equilibrium point.*

The following property present cases where the solution to the ODE system (1) converges to the zero state (depending on the initial condition).

Property 9. *In the CDM ODE system (1), suppose* $c_i = 1$ *and* $g_i = 0$ *for all* i. *Then the zero state is a stable equilibrium point when* $\rho_i > \beta_i / K_i$ *for all* i, *or an unstable equilibrium point when* $\rho_i < \beta_i / K_i$ *for at least one* i. *When* $\rho_i = \beta_i / K_i$ *for at least one* i, *then we have an attractor only if* X_i *is restricted to be non-negative and* $\rho_j \geq \beta_j / K_j$ *for every* $j \neq i$.

In addition, suppose $c_i > 1$, $\rho_i > 0$ *and* $g_i = 0$ *for all* i. *Then the zero state is a stable equilibrium point of the ODE system (1).*

Remark 2. Suppose $c_i > 1$, $\rho_i > 0$ and $g_i = 0$. Then $X_i^* = 0$ is always an attracting component.

Remark (2) is important because this suggests that if the i-th component is switched-off then it can never be switched-on again, unless we effectively perturb the system by introducing an additive external stimulus (s_i) or some stochastic noise [60, 61, 62, 63, 42, 64]. In some cases where a zero attracting

PeerJ PrePrints | http://dx.doi.org/10.7287/peerj.preprints.382v3 | CC-BY 4.0 Open Access | rec: 31 Jan 2015, publ: 31 Jan 2015

component is unwanted, a modified CDM ODE model can be used, such as

$$\frac{dX_i}{dt} = \frac{\beta_i \exp(c_i(X_i - \delta_i))}{K_i + \exp(c_i(X_i - \delta_i)) + \sum_{j \neq i} \gamma_{i,j} \exp(c_{i,j}(X_j - \delta_j))} + g_i - \rho_i X_i \text{ for } i = 1, 2, ..., n. \quad (15)$$

The parameter δ_i shifts the sigmoid kinetics of the i-th component to higher values of X_i. In cell differentiation [65, 66], the zero state has trivial biological importance because it does not represent any phenotype.

3.3. Several types of equilibrium switching

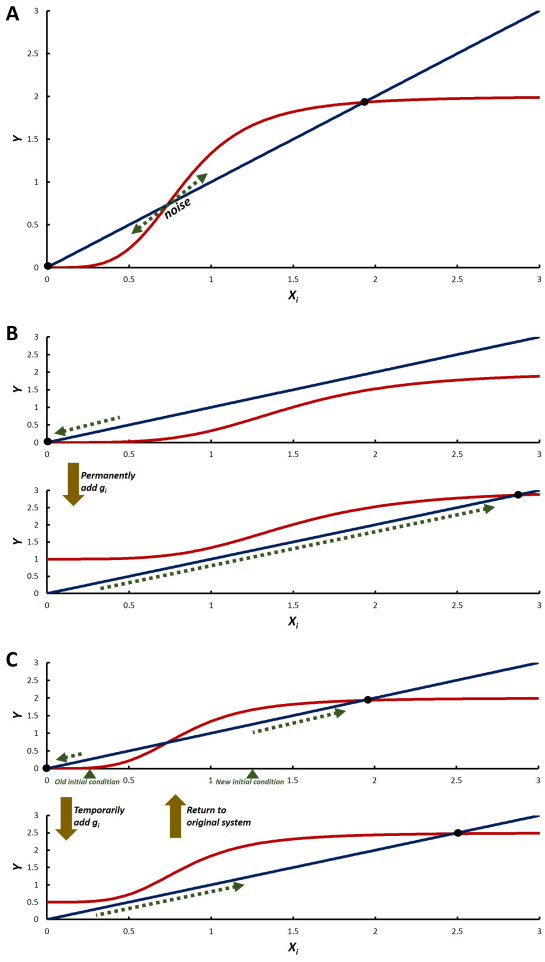

Figure 5: (**A**) Noise-driven equilibrium switching. (**B**) Switching by permanently changing a parameter value. (**C**) Switching by driving the solution to another basin of attraction through temporarily changing a parameter value.

Equilibrium switching from undesirable steady state to the desired steady state can happen without or with changing parameter values (parameter regulation). To explain the scenarios of switching, suppose $n = 1$ (see Figure (5)). Figure (5A) shows noise-driven switching without parameter regulation. This noise-driven switching is possible in a system with multi-stable states [67, 61, 63, 42, 68]. Figure (5B) is an example of switching by permanently changing a parameter value. On the other hand, Figure (5C) presents a strategy by temporarily varying the value of a parameter. This temporary change in parameter value drives the solution to the ODE model from one steady state's basin of attraction to another steady state's basin of attraction.

3.4. Illustrations of equilibrium switching by parameter regulation

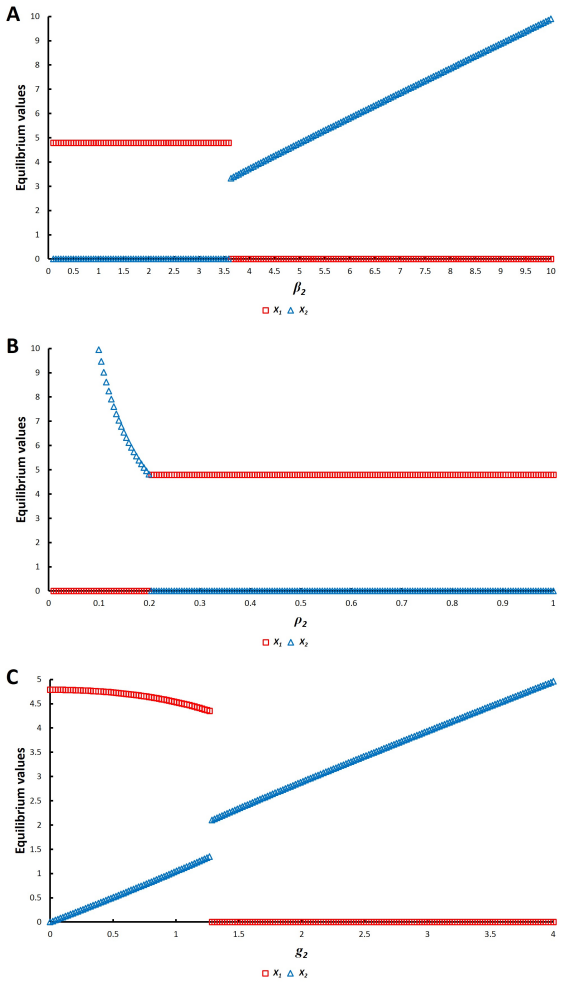

Figure 6: Let $n = 2$, $c_1 = c_2 = c_{1,2} = c_{2,1} = 1$, $\beta_1 = 1$, $K_1 = K_2 = 1$, $\gamma_{1,2} = \gamma_{2,1} = 1$, $\rho_1 = 0.2$ and $g_1 = 0$. (**A**) Varying the value of β_2 can switch equilibrium states. Initial values are set to $X_{1,0} = 1$ and $X_{2,0} = 1$, and parameter values are $\rho_2 = 1$ and $g_2 = 0$. (**B**) Varying the value of ρ_2 can switch equilibrium states. Initial values are set to $X_{1,0} = 1$ and $X_{2,0} = 1$, and parameter values are $\beta_2 = 1$ and $g_2 = 0$. (**C**) Varying the value of g_2 can switch equilibrium states even though the initial condition of X_2 is switched-off. Initial values are set to $X_{1,0} = 1$ and $X_{2,0} = 0$, and parameter values are $\beta_2 = 1$ and $\rho_2 = 1$.

We can mathematically manipulate the parameter values to ensure that the initial condition is in the basin of attraction of the desired steady state. We can do this by decreasing the size of the basin of attraction of an undesirable steady state as well as increasing the size of the basin of attraction of the desired steady state. For example, we can force the i-th component of a state to eventually dominate other components by increasing the

PeerJ PrePrints | http://dx.doi.org/10.7287/peerj.preprints.382v3 | CC-BY 4.0 Open Access | rec: 31 Jan 2015, publ: 31 Jan 2015

maximal growth rate $\beta_i + g_i$ [69, 70, 71, 72, 73] or by decreasing the decay rate ρ_i (Figure (6A-C)) [74, 75, 76, 77].

Here we assume that changes in external stimuli are represented by the variations in the parameter g_i. The parameter g_i is assumed as a constant production term that alters the minimum and maximum values of the multivariate sigmoid function. If we increase the value of g_i then the value of the attracting component X_i^* where $Y = H_i^1(X_i) + g_i$ and $Y = \rho_i(X_i)$ intersect also increases. In fact, we can force such enhanced value of X_i^* to be the only intersection even if the value of $\sum_{j \neq i} \gamma_{i,j} X_j^{c_{i,j}}$ increases (see Figure (7A) for illustration).

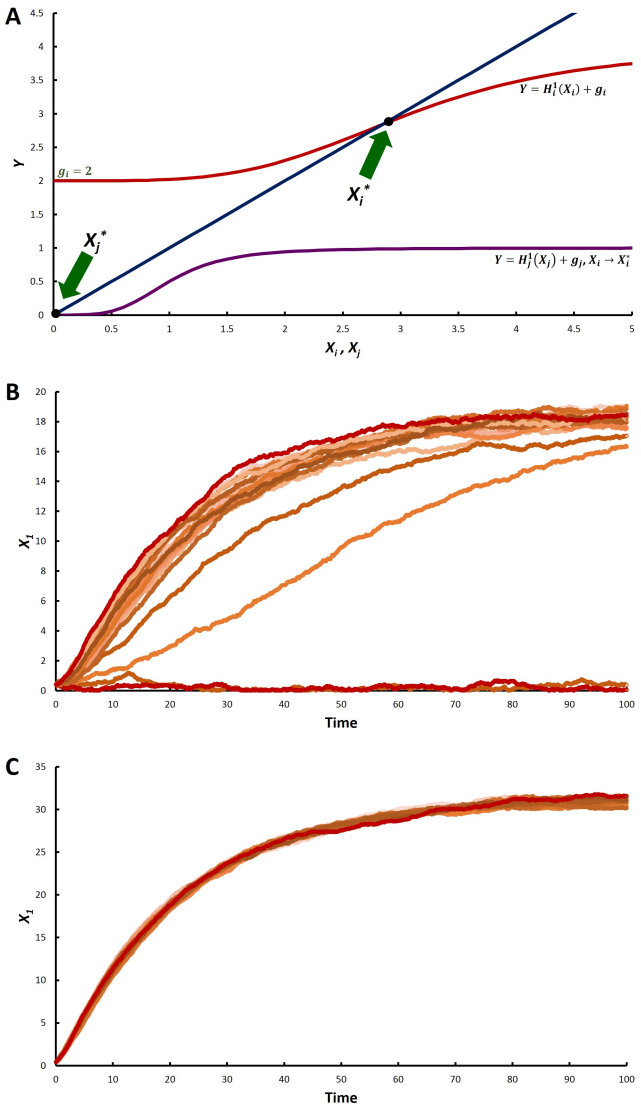

Figure 7: (**A**) Increasing the value of g_i can steer X_i to converge to the sole high-valued X_i^*, and X_j to converge to the sole low-valued X_j^*. (**B**) Let us consider the ODE model in Example (5) but set $g_1 = dW$ where dW is a Gaussian white noise (see [42]). Stochastic noise can drive sample paths to different steady states of the CDM ODE model. Out of the 20 simulation runs, 2 of the sample paths tend to the lower-valued attracting component. Initial condition is $(0.4, 0.5)$, only the sample paths of X_1 are shown in the figure. (**C**) Setting $g_1 = 0.5 + dW$, all sample paths out of the 20 simulation runs tend to the sole steady state of the CDM ODE model. Initial condition is $(0.4, 0.5)$, only the sample paths of X_1 are shown in the figure.

The component X_i inhibits X_j, hence, if we increase the value of X_i^* by adding g_i then the value of X_j^*, $j \neq i$ where $Y = H_j^1(X_j) + g_j$ and $Y = \rho_j(X_j)$ intersect decreases. We can actually force such decreased value of X_j^* to be the only intersection by amplifying g_i up to a sufficient level (note that if $g_j = 0$, then it is possible to make the switched-off $X_j^* = 0$ the only attracting component). Therefore, by sufficiently changing the value of g_i we can have a sole stable steady state where the i-th component dominates the others ($X_i^* > X_j^*$, $j \neq i$; a premier state). For any initial condition, the solution to the CDM ODE model (1) converges to this sole steady state (see Figure (7A) for an example).

The perpetual addition of sufficient amount of external stimulus, represented by constant g_i, can shut down the multi-stability of the system such that only one stable steady state remains. Thus, this strategy increases the robustness of the solution to the CDM ODE model against stochastic noise that induces equilibrium switching. Figure (7B) shows that stochastic noise can drive sample paths (solutions to stochastic differential equations) to different stable steady states of the CDM ODE model. However, adding a constant supply of external stimulus can minimize this noise-driven switching as illustrated in Figure (7C).

Here is an example that demonstrates the effect of parameter regulation on multi-stability:

Example 5. Consider the CDM ODE model (1) of the form:

$$\frac{dX_1}{dt} = \frac{X_1^2}{1 + X_1^2 + \frac{1}{8}X_2^2} - \frac{1}{21}X_1 \qquad (16)$$
$$\frac{dX_2}{dt} = \frac{X_2^2}{1 + \frac{1}{8}X_1^2 + X_2^2} - \frac{1}{21}X_2.$$

This system has 9 steady states which is equal to the Bézout upper bound (Property (5)). There are only 4 stable steady states out of the 9. The four stable steady states represent a priming state (2-node co-dominance), two premier states (1-node dominance) and a zero state (see Appendix B for the numerical results).

Now, suppose we introduce $g_1 = 0.5$. Introducing $g_1 = 0.5$ forces X_1 to converge to the high-valued attracting component X_1^*, and forces

$$\frac{X_2^2}{1 + \frac{1}{8}X_1^{*2} + X_2^2} < \frac{1}{21}X_2 \qquad (17)$$

for all values of X_2. Hence, there will be exactly one steady state. This steady state is stable and represents a premier state where X_1^* is dominant and X_2^* is switched-off.

On the other hand, the parameters K_i, c_i, $c_{i,j}$ and $\gamma_{i,j}$ do not affect the upper bound of the hyperspace (7). However, increasing K_j for all $j \neq i$ can force each X_j to converge to the lower-valued attracting component (or even be switched-off when $g_j = 0$). This increases the chance of X_i to converge to $X_i^* > X_j^*$ for all $j \neq i$. Furthermore, increasing the value

PeerJ PrePrints | http://dx.doi.org/10.7287/peerj.preprints.382v3 | CC-BY 4.0 Open Access | rec: 31 Jan 2015, publ: 31 Jan 2015

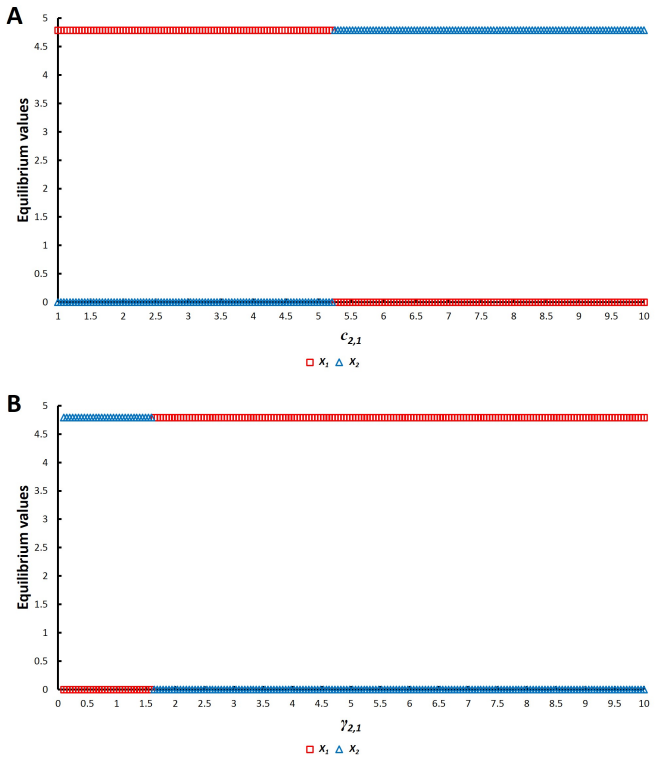

Figure 8: Increasing the inhibition exponent $c_{2,1}$ and interaction coefficient $\gamma_{2,1}$ can drive equilibrium switching. Let $n = 2$, $X_0 = (1, 1.2)$, $c_1 = c_2 = c_{1,2} = 2$, $\beta_1 = \beta_2 = 1$, $K_1 = K_2 = 1$, $\gamma_{1,2} = 1$, $\rho_1 = \rho_2 = 0.2$ and $g_1 = g_2 = 0$. (**A**) Varying the value of $c_{2,1}$. (**B**) Varying the value of $\gamma_{2,1}$.

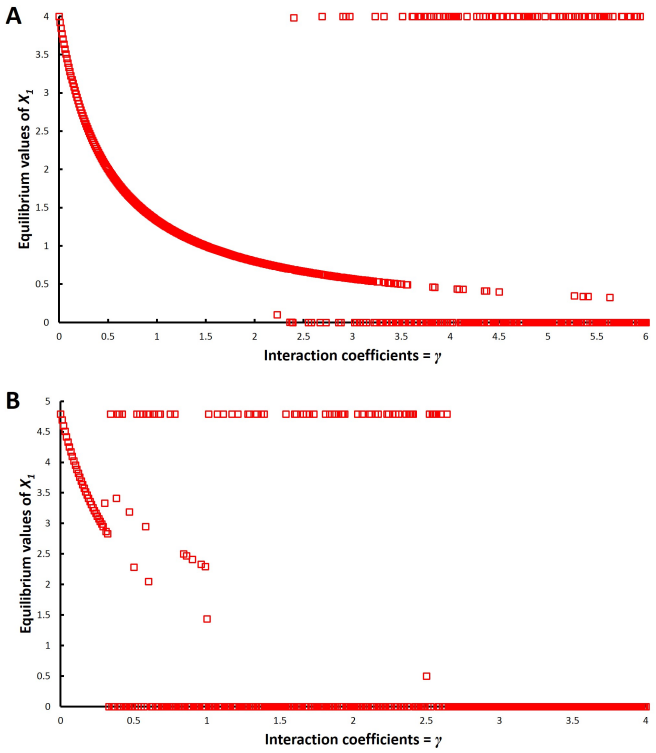

Figure 9: Varying the interaction coefficients can prompt steady state switching. Suppose $n = 3$, $X_0 \approx (0.5, 0.5, 0.5)$, $g_i = 0$, $\gamma_{i,j} = \gamma$, $\beta_i = 1$, $\rho_i = 0.2$ and $K_i = 1$, for all i, j. Only the equilibrium values of X_1 are shown. (**A**) Let $c_i = c_{i,j} = 1$ for all i, j. (**B**) Let $c_i = c_{i,j} = 2$ for all i, j.

of c_i or $c_{i,j}$ can result in an increased number of steady states (by Property (5)). Varying the values of these exponents can prompt steady state switching (Figure (8)) and can also result in oscillations (see Appendix A.2).

There are cases where the interaction coefficients ($\gamma_{i,j}$) act as controls to induce steady state switching. Increasing the inhibition strength of one component can affect its dominance over the other components. For example, recall the steady state in Example (3) for $n = 2$ with $c_i = c_{i,j} = 1$ and $g_i = 0$, $i, j = 1, 2$,

$$\left(\frac{\beta_1 - \rho_1 \left(K_1 + \gamma_{1,2} {X_2}^*\right)}{\rho_1}, \frac{\beta_2 - \rho_2 \left(K_2 + \gamma_{2,1} {X_1}^*\right)}{\rho_2}\right). \qquad (18)$$

Notice that as we enhance the inhibition of X_1 by X_2, represented by $\gamma_{1,2}$, it can drive $\beta_1 < \rho_1 \left(K_1 + \gamma_{1,2} {X_2}^*\right)$ that switches-off ${X_1}^*$. This drives X_2 to eventually dominate X_1.

The diagrams in Figure (9) present additional illustrations of steady state switching by varying the value of the interaction coefficients. However, regulating the interaction among components is not always as straightforward as regulating the values of β_i, g_i and ρ_i in steering the system toward the desired steady state. Having an asymmetric interaction matrix can generate oscillating behavior, such as the repressilator (Appendix A.1).

Oscillations can lead to state switching for some period of time. If the solution attains a desired temporal condition, we can dampen the oscillating behavior (e.g., by parameter regulation from asymmetric to symmetric $[\gamma_{i,j}]$) to have stability where the desired outcome is maintained (Appendix C). This is a strategy where oscillations and stability both assist in driving a solution towards the desired equilibrium [78]. To avoid volatile effect of randomness, the oscillation-driven switching can be an alternative to the the noise-driven switching but only when oscillation is structurally feasible.

4. Conclusions

Mathematical models, although simpler than the real multifaceted system, can provide insights on the different possible outcomes arising from the interaction of the components. We are able to show the qualitative dynamics of the concurrent decision-making model (CDM) by investigating the mathematical properties of its associated system of ordinary differential equations (ODE) with nonlinear kinetics. The CDM can predict multi-stability that may give rise to co-existence or to domination by some components. Regulating the maximal growth rate (which is possibly influenced by an external stimulus), decay rate, and interaction among components can affect the nature of the steady states. Parameter regulation is a possible deterministic strategy for controlling the dominance of a component towards the desired steady state. The introduction of an external stimulus can result in a system with a sole attractor, which can control the effect of moderate stochastic noise.

In some cases, CDM can also represent synthetic biological oscillators. Combining the effect of oscillation and stability can

PeerJ PrePrints | http://dx.doi.org/10.7287/peerj.preprints.382v3 | CC-BY 4.0 Open Access | rec: 31 Jan 2015, publ: 31 Jan 2015

be a potential strategy for attaining the desired outcome. Asymmetric reciprocal strength of inhibition among components can result in sustained oscillations, but this is not true for all asymmetric systems. Our study can be extended to search for general conditions that generate oscillatory behavior, and to determine if the CDM can exhibit chaos, such as in the presence of delay.

If we want to reactivate a switched-off component then one strategy is to add an external stimulus that enhances the basal growth. However, it is sometimes impractical or infeasible to continuously add such a constant amount of inducement. Consequently, we may rather consider an external stimulus that varies through time. If there are multiple stable steady states, introducing a varying amount of stimulus can affect the long-term outcome of the CDM dynamics through equilibrium switching. If deterministic parameter regulation is not perpetually possible, combining deterministic and stochastic techniques could be done, such as by supplementing the effect of external stimulus with stochastic fluctuations.

Supplementary Material

For the proofs of the mathematical properties and additional illustrations, see the supporting text in the Supplementary Material.

Acknowledgment

This work was financially supported by the Philippine Council for Industry, Energy and Emerging Technology Research and Development (PCIEERD) of the Department of Science and Technology (DOST), and by the University of the Philippines. We express our sincere thanks to Baltazar D. Aguda and Ariel L. Babierra for the useful discussion and comments.

Declarations: The authors declare that there are no conflicts of interest. The funding sources had no involvement in the study design, in the analysis and interpretation of results, in the writing of the manuscript and in the decision to submit the article for publication.

References

[1] B. Barzel, A.-L. Barabasi, Universality in network dynamics, Nature Phys. 9 (2013) 673–681. doi:10.1038/nphys2741.

[2] Y.-Y. Liu, J.-J. Slotine, A.-L. Barabasi, Observability of complex systems, PNAS 110 (7) (2013) 2460–2465. doi:10.1073/pnas.1215508110.

[3] F. S. Neves, M. Timme, Computation by switching in complex networks of states, Phys. Rev. Lett. 109 (2012) 018701. doi:10.1103/PhysRevLett.109.018701.

[4] H. Neumeister, K. W. Whitaker, H. A. Hofmann, T. Preuss, Social and ecological regulation of a decision-making circuit, J. Neurophysiol. 104 (6) (2010) 3180–3188. doi:10.1152/jn.00574.2010.

[5] S. Boccaletti, V. Latora, Y. Moreno, M. Chavez, D.-U. Hwang, Complex networks: Structure and dynamics, Phys. Rep. 424 (2006) 175–308. doi:10.1016/j.physrep.2005.10.009.

[6] J. Panovska-Griffiths, K. M. Page, J. Briscoe, A gene regulatory motif that generates oscillatory or multiway switch outputs, J. R. Soc. Interface 10 (79) (2012) 20120826. doi:10.1098/rsif.2012.0826.

[7] B. L. Baumgartner, M. R. Bennett, M. Ferry, T. L. Johnson, L. S. Tsimring, J. Hasty, Antagonistic gene transcripts regulate adaptation to new growth environments, PNAS 108 (52) (2011) 21087–21092. doi:10.1073/pnas.1111408109.

[8] E. H. Davidson, Emerging properties of animal gene regulatory networks, Nature 468 (2010) 911–920. doi:10.1038/nature09645.

[9] J. Macia, S. Widder, R. Sole, Why are cellular switches boolean? general conditions for multistable genetic circuits, J. Theor. Biol. 261 (2009) 126–135. doi:10.1016/j.jtbi.2009.07.019.

[10] R. Guantes, J. F. Poyatos, Multistable decision switches for flexible control of epigenetic differentiation, PLoS Comput. Biol. 4 (11) (2008) e1000235. doi:10.1371/journal.pcbi.1000235.

[11] V. Chickarmane, C. Troein, U. A. Nuber, H. M. Sauro, C. Peterson, Transcriptional dynamics of the embryonic stem cell switch, PLoS Comput. Biol. 2 (9) (2006) e123. doi:10.1371/journal.pcbi.0020123.

[12] E. Kaarlejarvi, J. Olofsson, Concurrent biotic interactions influence plant performance at their altitudinal distribution margins, Oikos (2014) (online)doi:10.1111/oik.01261.

[13] G. Huguet, J. Rinzel, J. Hupe, Noise and adaptation in multistable perception: noise drives when to switch, adaptation determines percept choice, J. Vis. 14 (3) (2014) 1–24. doi:10.1167/14.3.19.

[14] A. Mougi, M. Kondoh, Diversity of interaction types and ecological community stability, Science 337 (2012) 349–351. doi:10.1126/science.1220529.

[15] S. B. Jeswiet, S. S. Lee-Jenkins, J.-G. J. Godin, Concurrent effects of sperm competition and female quality on male mate choice in the trinidadian guppy (*Poecilia reticulata*), Behav. Ecol. 23 (1) (2011) 195–200. doi:10.1093/beheco/arr175.

[16] N. Ganguly, A. Deutsch, A. Mukherjee (Eds.), Dynamics On and Of Complex Networks: Applications to Biology, Computer Science, and the Social Sciences, Birkhauser, Boston, 2009.

[17] O. Cinquin, J. Demongeot, High-dimensional switches and the modelling of cellular differentiation, J. Theor. Biol. 233 (2005) 391–411. doi:10.1016/j.jtbi.2004.10.027.

[18] A. N. Pisarchik, U. Feudel, Control of multistability, Phys. Rep. (2014) (online)doi:10.1016/j.physrep.2014.02.007.

[19] B. Luna, E. Galan-Vasquez, E. Ugalde, A. Martinez-Antonio, Structural comparison of biological networks based on dominant vertices, Mol. Biosyst. 9 (2013) 1765–1773. doi:10.1039/c3mb70077a.

[20] N. J. Cowan, E. J. Chastain, D. A. Vilhena, J. S. Freudenberg, C. T. Bergstrom, Nodal dynamics, not degree distributions, determine the structural controllability of complex networks, PLoS ONE 7 (6) (2012) e38398. doi:10.1371/journal.pone.0038398.

[21] S. Smale, On the differential equations of species in competition, J. Math. Biol. 3 (1) (1976) 5–7. doi:10.1007/BF00307854.

[22] Q. Zhang, S. Bhattacharya, M. E. Andersen, Ultrasensitive response motifs: basic amplifiers in molecular signalling networks, Open Biol. 3 (2013) 130031. doi:10.1098/rsob.130031.

[23] M. E. Andersen, R. S. H. Yang, C. T. French, L. S. Chubb, J. E. Dennison, Molecular circuits, biological switches, and nonlinear dose-response relationships, Environ. Health Perspect. 110 (Suppl 6) (2002) 971–978.

[24] R. Ranaldi, S. Ferguson, R. J. Beninger, Automating the generation and collection of rate-frequency functions in a curve-shift brain stimulation reward paradigm, J. Neurosci. Methods 53 (2) (1994) 163–172. doi:10.1016/0165-0270(94)90174-0.

[25] P. C. Faucon, K. Pardee, R. M. Kumar, H. Li, Y.-H. Loh, X. Wang, Gene networks of fully connected triads with complete auto-activation enable multistability and stepwise stochastic transitions, PLoS ONE 9 (7) (2014) e102873. doi:10.1371/journal.pone.0102873.

[26] A. Chatterjee, Y. N. Kaznessis, W.-S. Hu, Tweaking biological switches through a better understanding of bistability behavior, Curr. Opin. Biotechnol. 19 (5) (2008) 475–481. doi:10.1016/j.copbio.2008.08.010.

[27] J. J. Tyson, R. Albert, A. Goldbeter, P. Ruoff, J. Sible, Biological switches and clocks, J. R. Soc. Interface 5 (Suppl 1) (2008) S1–S8. doi:10.1098/rsif.2008.0179.focus.

[28] J. L. Cherry, F. R. Adler, How to make a biological switch, J. Theor. Biol. 203 (2) (2000) 117–133. doi:10.1006/jtbi.2000.1068.

[29] P. Smolen, D. A. Baxter, J. H. Byrne, Frequency selectivity, multistability, and oscillations emerge from models of genetic regulatory systems, Am. J. Physiol. 274 (1998) C531–C542.

[30] G. Li, H. Rabitz, Analysis of gene network robustness based on saturated fixed point attractors, EURASIP J. Bioinform. Syst. Biol. 2014 (4). doi:10.1186/1687-4153-2014-4.

[31] D. Angeli, J. E. Ferrel, Jr., E. D. Sontag, Detection of multistability, bifurcations, and hysteresis in a large class of biological positive-feedback systems, PNAS 101 (7) (2004) 1822–1827. doi:10.1073/

pnas.0308265100.
[32] A. Tsoularis, J. Wallace, Analysis of logistic growth models, Math. Biosci. 179 (1) (2002) 21–55. doi:10.1016/S0025-5564(02)00096-2.
[33] M. Laurent, N. Kellershohn, Multistability: a major means of differentiation and evolution in biological systems, Trends Biochem. Sci. 24 (11) (1999) 418–422. doi:10.1016/S0968-0004(99)01473-5.
[34] W. L. Kath, J. D. Murray, Analysis of a model biological switch, SIAM J. Appl. Math. 45 (6) (1985) 943–955. doi:10.1137/0145057.
[35] B. D. Aguda, A. Friedman, Models of Cellular Regulation, Oxford University Press, NY, 2008.
[36] S. DeDeo, D. C. Krakauer, Dynamics and processing in finite self-similar networks, J. R. Soc. Interface (2012) (online)doi:10.1098/rsif.2011.0840.
[37] D. Siegal-Gaskins, M. K. Mejia-Guerra, G. D. Smith, E. Grotewold, Emergence of switch-like behavior in a large family of simple biochemical networks, PLoS Comput. Biol. 7 (5) (2011) e1002039. doi:10.1371/journal.pcbi.1002039.
[38] J. J. Tyson, B. Novak, Functional motifs in biochemical reaction networks, Annu. Rev. Phys. Chem. 61 (2010) 219–240. doi:10.1146/annurev.physchem.012809.103457.
[39] A. Mochizuki, An analytical study of the number of steady states in gene regulatory networks, J. Theor. Biol. 236 (3) (2005) 291 – 310. doi:10.1016/j.jtbi.2005.03.015.
[40] P. Brazhnik, A. de la Fuente, P. Mendez, Gene networks: how to put the function in genomics, Trends Biotechnol. 20 (11) (2002) 467–472. doi:10.1016/S0167-7799(02)02053-X.
[41] R. Milo, S. Shen-Orr, S. Itzkovitz, N. Kashtan, D. Chklovskii, U. Alon, Network motifs: Simple building blocks of complex networks, Science 298 (2002) 824–827. doi:10.1126/science.298.5594.824.
[42] B. D. MacArthur, C. P. Please, R. O. C. Oreffo, Stochasticity and the molecular mechanisms of induced pluripotency, PLoS ONE 3 (8) (2008) e3086. doi:10.1371/journal.pone.0003086.
[43] M. Andrecut, Monte-carlo simulation of a multi-dimensional switch-like model of stem cell differentiation, in: C. J. Mode (Ed.), Applications of Monte Carlo Methods in Biology, Medicine and Other Fields of Science, InTech, 2011, Ch. 2, pp. 25–40. doi:10.5772/15474.
[44] W. F. Boss, H. W. Sederoff, Y. J. Im, N. Moran, A. M. Grunden, I. Y. Perera, Basal signaling regulates plant growth and development, Plant Physiol. 154 (2) (2010) 439–443. doi:10.1104/pp.110.161232.
[45] T. Juven-Gershon, J. T. Kadonaga, Regulation of gene expression via the core promoter and the basal transcriptional machinery, Dev. Biol. 339 (2) (2010) 225–229. doi:10.1016/j.ydbio.2009.08.009.
[46] S. Goutelle, M. Maurin, F. Rougier, X. Barbaut, L. Bourguignon, M. Ducher, P. Maire, The hill equation: a review of its capabilities in pharmacological modelling, Fundam. Clin. Pharm. 22 (6) (2008) 633–648. doi:10.1111/j.1472-8206.2008.00633.x.
[47] M. Santillan, On the use of the hill functions in mathematical models of gene regulatory networks, Math. Model Nat. Phenom. 3 (2) (2008) 85–97. doi:10.1051/mmnp:2008056.
[48] J. X. Zhou, L. Brusch, S. Huang, Predicting pancreas cell fate decisions and reprogramming with a hierarchical multi-attractor model, PLoS ONE 6 (3) (2011) e14752. doi:10.1371/journal.pone.0014752.
[49] R. Dilao, The regulation of gene expression in eukaryotes: bistability and oscillations in repressilator models, J. Theor. Biol. (2014) (online)doi:10.1016/j.jtbi.2013.09.010.
[50] A. Kuznetsov, V. Afraimovich, Heteroclinic cycles in the repressilator model, Chaos Soliton. Fract. 45 (5) (2012) 660–665. doi:10.1016/j.chaos.2012.02.009.
[51] O. Buse, R. Perez, A. Kuznetsov, Dynamical properties of the repressilator model, Phys. Rev. E 81 (6) (2010) 066206. doi:10.1103/PhysRevE.81.066206.
[52] O. Purcell, N. J. Savery, C. S. Grierson, M. di Bernardo, A comparative analysis of synthetic genetic oscillators, J. R. Soc. Interface 7 (52) (2010) 1503–1524. doi:10.1098/rsif.2010.0183.
[53] S. Muller, J. Hofbauer, L. Endler, C. Flamm, S. Widder, P. Schuster, A generalized model of the repressilator, J. Math. Biol. 53 (6) (2006) 905–937. doi:10.1007/s00285-006-0035-9.
[54] M. B. Elowitz, S. Leibler, A synthetic oscillatory network of transcriptional regulators, Nature 403 (2000) 335–338. doi:10.1038/35002125.
[55] M. A. Leite, Y. Wang, Multistability, oscillations and bifurcations in feedback loops, Math. Biosci. Eng. 7 (1) (2010) 83–97. doi:10.3934/mbe.2010.7.83.
[56] N. Radde, The role of feedback mechanisms in biological network models, Asian J. Control 13 (5) (2011) 597–610. doi:10.1002/asjc.376.
[57] M. Mincheva, G. Craciun, Multigraph conditions for multistability, oscillations and pattern formation in biochemical reaction networks, P. IEEE 96 (8) (2008) 1281–1291. doi:10.1109/JPROC.2008.925474.
[58] D. Thieffry, Dynamical roles of biological regulatory circuits, Brief. Bioinform. 8 (4) (2002) 220–225. doi:10.1093/bib/bbm028.
[59] E. Bezout, Théorie générale des équations algébriques, Paris, Impr. de P.-D. Pierres, Paris, 1779.
[60] T. S. Macfarlan, W. D. Gifford, S. Driscoll, K. Lettieri, H. M. Rowe, D. Bonanomi, A. Firth, O. Singer, D. Trono, S. L. Pfaff, Embryonic stem cell potency fluctuates with endogenous retrovirus activity, Nature 487 (2012) 57–63. doi:10.1038/nature11244.
[61] K. H. Kim, H. M. Sauro, Adjusting phenotypes by noise control, PLoS Comput. Biol. 8 (1) (2012) e1002344. doi:10.1371/journal.pcbi.1002344.
[62] E. Pujadas, A. P. Feinberg, Regulated noise in the epigenetic landscape of development and disease, Cell 148 (6) (2012) 1123–1131. doi:10.1016/j.cell.2012.02.045.
[63] S. Yamanaka, Elite and stochastic models for induced pluripotent stem cell generation, Nature 460 (2009) 49–52. doi:10.1038/nature08180.
[64] H. H. Chang, M. Hemberg, M. Barahona, D. E. Ingber, S. Huang, Transcriptome-wide noise controls lineage choice in mammalian progenitor cells, Nature 453 (2008) 544–548. doi:10.1038/nature06965.
[65] S. Huang, The molecular and mathematical basis of waddington's epigenetic landscape: a framework for post-darwinian biology?, Bioessays 34 (2) (2011) 149–157. doi:10.1002/bies.201100031.
[66] S. Huang, Cell lineage determination in state space: A systems view brings flexibility to dogmatic canonical rules, PLoS Biol. 8 (5) (2010) e1000380. doi:10.1371/journal.pbio.1000380.
[67] M. Chen, L. Wang, C. C. Liu, Q. Nie, Noise attenuation in the on and off states of biological switches, ACS Synth. Biol. 2 (10) (2013) 587–593. doi:10.1021/sb400044g.
[68] J. Wang, J. Zhang, Z. Yuan, T. Zhou, Noise-induced switches in network systems of the genetic toggle switch, BMC Syst. Biol. 1 (2007) 50. doi:10.1186/1752-0509-1-50.
[69] S. Masuda, J. Wu, T. Hishida, G. N. Pandian, H. Sugiyama, J. C. Izpisua Belmonte, Chemically induced pluripotent stem cells (cipscs): a transgene-free approach, J. Mol. Cell Biol. 5 (5) (2013) 354–355. doi:10.1093/jmcb/mjt034.
[70] P. Hou, Y. Li, X. Zhang, C. Liu, J. Guan, H. Li, T. Zhao, J. Ye, W. Yang, K. Liu, J. Ge, J. Xu, Q. Zhang, Y. Zhao, H. Deng, Pluripotent stem cells induced from mouse somatic cells by small-molecule compounds, Science 341 (6146) (2013) 651–654. doi:10.1126/science.1239278.
[71] G. N. Pandian, H. Sugiyama, Programmable genetic switches to control transcriptional machinery of pluripotency, Biotechnology Journal 7 (6) (2012) 798–809. doi:10.1002/biot.201100361.
[72] M. F. Pera, P. P. L. Tam, Extrinsic regulation of pluripotent stem cells, Nature 465 (2010) 713–720. doi:10.1038/nature09228.
[73] V. M. Weake, J. L. Workman, Inducible gene expression: diverse regulatory mechanisms, Nature Reviews Genetics 11 (2010) 426–437. doi:10.1038/nrg2781.
[74] R. Hanel, M. Pochacker, M. Scholling, S. Thurner, A self-organized model for cell-differentiation based on variations of molecular decay rates, PLoS ONE 7 (5) (2012) e36679. doi:10.1371/journal.pone.0036679.
[75] P. A. C. 't Hoen, M. Hirsch, E. J. d. Meijer, R. X. d. Menezes, G. J. van Ommen, J. T. d. Dunnen, mrna degradation controls differentiation state-dependent differences in transcript and splice variant abundance, Nucleic Acids Res. 39 (2) (2011) 556–566. doi:10.1093/nar/gkq790.
[76] J. Houseley, D. Tollervey, The many pathways of rna degradation, Cell 136 (2009) 763–776. doi:10.1016/j.cell.2009.01.019.
[77] R. Xu, M. A. J. Chaplain, F. A. Davidson, Modelling and analysis of a competitive model with stage structure, Math. Comput. Model. 41 (2-3) (2005) 159–175. doi:10.1016/j.mcm.2004.08.003.
[78] N. Suzuki, C. Furusawa, K. Kaneko, Oscillatory protein expression dynamics endows stem cells with robust differentiation potential, PLoS ONE 6 (11) (2011) e27232. doi:10.1371/journal.pone.0027232.

PeerJ PrePrints | http://dx.doi.org/10.7287/peerj.preprints.382v3 | CC-BY 4.0 Open Access | rec: 31 Jan 2015, publ: 31 Jan 2015

Appendix A. Examples of Oscillators

Appendix A.1. Repressilator in Example (2)

The network representation and matrix of the interaction coefficients of the CDM system in Example (2) are shown in Figure (A.10A). Notice that one direction of inhibition is stronger than the reverse direction. This network is an example of a negative circuit forming a repressilator.

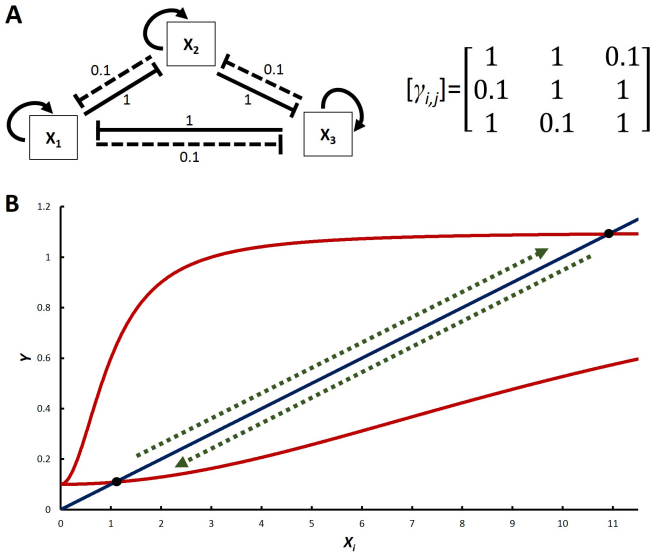

Figure A.10: (**A**) Network representation and matrix of the interaction coefficients of the CDM system in Example (2). Solid bars represent strong inhibition, broken bars represent weak inhibition. (**B**) The two sigmoid curves are sample graphs of $Y = H_i^1(X_i)$ with different values of X_j, $j \neq i$. The denominator of the sigmoid function H_i, $i = 1, 2, 3$ in the CDM model in Example (2) continuously varies resulting in oscillations. The oscillating solution to X_i is sequentially attracted by high-valued and low-valued attracting components.

The CDM ODE model in Example (2) does not have stable steady states. In fact, there is only one steady state, $X^* = (5.693, 5.693, 5.693)$, but it is unstable. However, each component $X_i^* = 5.693$ is attracting. Property (1) cannot be used to determine the stability of this steady state. Note that if the initial condition $X_{10} = X_{20} = X_{30}$, the solution converges to this sole steady state; but for other initial conditions, oscillations may persist.

Furthermore, the attracting components of every state contribute in the generation of the oscillating behavior (see Figure (A.10B) for illustration).

Appendix A.2. CDM system with asymmetric matrix of inhibition exponents

Another example of an oscillator arising from the asymmetric reciprocal inhibitory interaction of the components is of the following form

$$\begin{aligned}
\frac{dX_1}{dt} &= \frac{X_1^2}{1 + X_1^2 + X_2^3 + X_3} - 0.1X_1 + 0.1 \qquad \text{(A.1)}\\
\frac{dX_2}{dt} &= \frac{X_2^2}{1 + X_1 + X_2^2 + X_3^3} - 0.1X_2 + 0.1\\
\frac{dX_3}{dt} &= \frac{X_3^2}{1 + X_1^3 + X_2 + X_3^2} - 0.1X_3 + 0.1.
\end{aligned}$$

Notice that the matrix of inhibition exponents $[c_{i,j}]$ is asymmetric.

Appendix B. Numerical results for Example (5)

The approximate values of the steady states of the ODE system (16) in Example (5) are (also see Figure (B.11))

$(X_1^* = 18.619, X_2^* = 18.619)$ — stable (priming state),
$(X_1^* = 20.894, X_2^* = 3.1056)$ — unstable,
$(X_1^* = 3.1056, X_2^* = 20.894)$ — unstable,
$(X_1^* = 0.047741, X_2^* = 0.047741)$ — unstable,
$(X_1^* = 0, X_2^* = 0.047728)$ — unstable,
$(X_1^* = 0.047728, X_2^* = 0)$ — unstable,
$(X_1^* = 0, X_2^* = 20.952)$ — stable (premier state),
$(X_1^* = 20.952, X_2^* = 0)$ — stable (premier state), and
$(X_1^* = 0, X_2^* = 0)$ — stable (zero state).

If $g_1 = 0.5$ is introduced, the sole equilibrium is $(X_1^* = 31.479, X_2^* = 0)$.

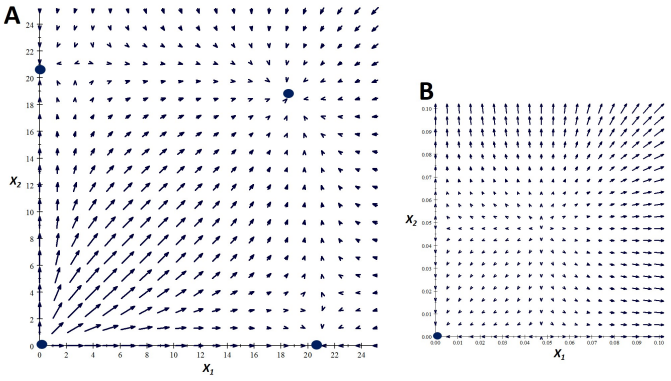

Figure B.11: (**A**) A phase plane showing the steady states of the ODE system (16) in Example (5), $g_1 = 0$. (**B**) Zooming in to show zero state is also stable.

Appendix C. Stabilizing oscillations

Consider the following oscillating system

$$\begin{aligned}
\frac{dX_1}{dt} &= \frac{X_1^2}{1 + X_1^2 + X_2^2 + 0.1X_3^2} - 0.1X_1 + 0.1 \qquad \text{(C.1)}\\
\frac{dX_2}{dt} &= \frac{X_2^2}{1 + 0.1X_1^2 + X_2^2 + X_3^2} - 0.1X_2 + 0.1\\
\frac{dX_3}{dt} &= \frac{X_3^2}{1 + X_1^2 + \phi X_2^2 + X_3^2} - 0.1X_3 + 0.1.
\end{aligned}$$

PeerJ PrePrints | http://dx.doi.org/10.7287/peerj.preprints.382v3 | CC-BY 4.0 Open Access | rec: 31 Jan 2015, publ: 31 Jan 2015

where $\phi = 0.1$ with initial condition $X_0 = (5, 1, 5)$. If we vary ϕ by setting

$$\frac{d\phi}{dt} = \frac{1}{1000(1 + \phi^2)} \tag{C.2}$$

with initial value of ϕ equal to 0.1, this would lead to stabilized oscillation towards dominant $X_2{}^*$ (Figure (C.12)).

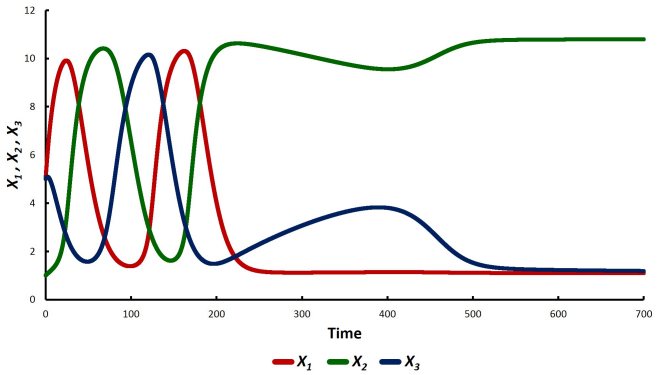

Figure C.12: An example of a controlled oscillating system by regulating an interaction coefficient. X_2 is initially inferior but eventually becomes dominant.

PeerJ PrePrints | http://dx.doi.org/10.7287/peerj.preprints.382v3 | CC-BY 4.0 Open Access | rec: 31 Jan 2015, publ: 31 Jan 2015